PAPER

Check for updates

Chiral Cu(II), Co(II) and Ni(II) complexes based on 2,2′-bipyridine modified peptoids†

Maria Baskin and Galia Maayan (ID) *

Helical peptoids bearing 2,2′-bipyridine, varied in their chiral bulky side chains and their N-terminus form complexes with Cu(II), Co(II) and Ni(II) *via* intramolecular binding. Chiral induction from the peptoid to each metal center could be only observed in some cases and is dependent on the identity of the N-terminus and on its position relative to the metal center.

Introduction

Chirality is a fundamental biological and chemical property, which plays a significant role in processes such as molecular recognition, regulation and catalysis. In nature, these processes are facilitated by efficient transfer of chiral information from the chiral backbone of peptides and biopolymers to embedded reactive centers including metal complexes. Achieving stereo-chemical control within synthetic systems is therefore a key to the development of bio-inspired functional molecules. In nature, induction of chirality to metal centers is directly related to information transfer from chiral ligands or chiral scaffolds. Synthetically, this can be accomplished by a rational design of an asymmetric inducing environment,[1] such as the one provided by folded macromolecules,[2] oligomers that can fold upon non-covalent interactions (foldamers),[3,4] and helical peptide mimics.[5] The biomimetic design of artificial chiral inductive systems for achieving total control over the stereochemistry of metal complexes is an important step towards applications in drug design,[6] recognition,[7] sensing[8] and asymmetric catalysis.[9]

"Peptoids", *N*-substituted glycine oligomers, are synthetic peptide mimics that benefit from the sequence specificity of biopolymers, on one hand, and from high stability and chemical diversity of synthetic polymers, on the other hand.[10] Peptoids can be easily and efficiently synthesized on solid support from primary amines *via* acylation followed by amine displacement to form *N*-substituted oligomers.[11] This repetitive two-steps synthetic method enables the incorporation of various functional groups as side-chains. In addition, peptoids can adopt stable helical conformations in solution[12] if chiral aromatic or tertiary butyl groups, are incorporated within their backbone.[13,14] The secondary structure is forced due to steric and electronic interactions and resembles this of polyproline type I (PPI) helix with approximately three residues per turn. In recent years, metallopeptoids,[15,16] as well as other metallo-foldamers[17] have received much attention due to their high potency to mimic the structure and function of natural metalloproteins. Specifically, we have recently described the transfer of chirality from either chiral helical or chiral unstructured peptoid scaffolds to embedded achiral metal centers, including Cu^{2+} or Co^{2+} complexes from 8-hydroxyquinoline[18,19] and Ru^{2+} complexes from 2,2′-bipyridine (bipy).[16] In the latter example, we have demonstrated that chiral induction from peptoid backbones to an embedded achiral Ru(bipy)$_3$ center lead to chiral Ru(bipy)$_3$ complexes with a preferable stereochemistry of the Δ isomers over the Λ isomers.

Herein, we explored the coordination of the biologically relevant metal ions Cu^{2+}, Co^{2+} and Ni^{2+} to several bipy-modified linear and cyclic peptoid sequences, varied in their chiral bulky side chains that are either aromatic (phenylethyl, naphtylethyl) or aliphatic (3,3-dimethyl-2-butyl), in their oligomer length, and in their N-terminus. We investigated the transfer of chiral information from the peptoid scaffold, which provides an asymmetric environment about the metal center, to the achiral metal complexes. We have discovered that chiral induction from each peptoid to each metal center is dependent on the coordination environment of the metal center, which is a result of both the identity of the N-terminus (amine or amide) and its location in the sequence relative to the metal center.

Results and discussion

Initially, two linear helical peptoid hexamers, **L2B** and **R-L2B**, bearing two bipy ligands at the 2nd and 5th positions and four chiral phenyl ethyl groups (*S* or *R* respectively) in the other positions, as well as two cyclic helical peptoid hexamers, **C3B**

Schulich Faculty of Chemistry, Technion-Israel Institute of Technology, Haifa, 3200003, Israel. E-mail: gm92@tx.technion.ac.il

and **R-C3B**, bearing three bipy ligands and three chiral phenyl ethyl groups (*S* or *R* respectively) in alternating positions were prepared and characterized (Fig. 1a).[16] These peptoids were expected to form intramolecular complexes with each of the metal ions Cu^{2+}, Co^{2+} or Ni^{2+} (Fig. 1a). All the complexes in this study were prepared and analyzed in solution only. It is therefore possible that metallopeptoid complexes bearing two bipy ligands have additional coordinated solvent molecule(s) bound to the metal center. Metal free **L2B** peptoid exhibits absorption band near $\lambda = 299$ nm in acetonitrile solution that corresponds to the $\pi-\pi^*$ transitions of the bipy units. Titrating it with Cu^{2+} ions, produced a new absorption band at $\lambda = 315$ nm, indicating the formation of a copper-peptoid complex (Fig. 2a). From the UV-Vis titration we constructed a metal-to-peptoid ratio plot where a plateau was obtained at the molar ratio of 1 (Fig. 2a, inset). This could suggest either the formation of an intramolecular complex, with a ratio of 1 : 1 Cu^{2+} :

L2B, or an intermolecular complex with a ratio of 2 : 2 Cu^{2+} : **L2B**. Keeping the total molar concentration of a mixture solution, which contains both Cu^{2+} and **R-L2B**, constant at 33 μM and varying their mole fraction, a Job plot experiment was also conducted. The absorbance proportional to complex formation was plotted against the mole fraction and from the intersection point a stoichiometry ratio was determined to be 0.96,[20] supporting the metal-to-peptoid ratio obtained from the UV titrations.[21] Further on, ESI-MS analysis confirmed that the metal-to-peptoid ratio in this complex is 1 : 1, indicating the formation of an intramolecular Cu(**R-L2B**) complex. Similar UV-Vis titration experiments were conducted with **L2B**, **R-L2B**, **C3B** and **R-C3B** and the metal ions Cu^{2+}, Co^{2+} and Ni^{2+}. In most cases, a metal-to-peptoid ratio of 1 : 1 was obtained. In the cases of Ni(**L2B**) and Ni(**C3B**), however, a 1 : 1 was not obtained and therefore we have performed the corresponding Job plot experiments. From the intersection points, the stoi-
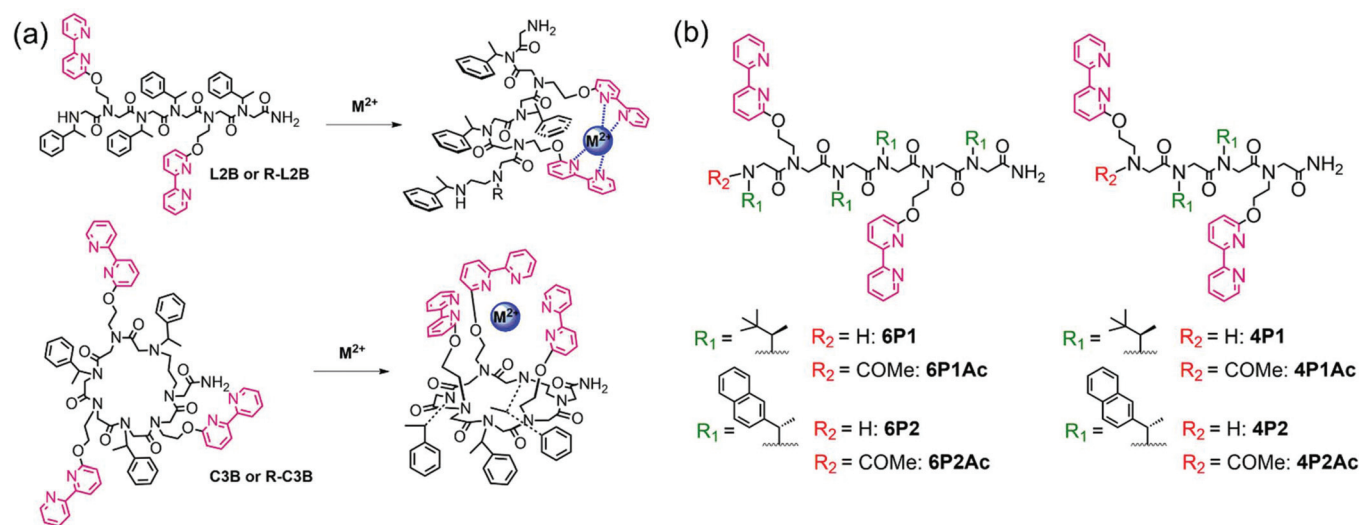

Fig. 1 Chemical structure of peptoid oligomers (a) **L2B**, **R-L2B**, **C3B**, **R-C3B** and their expected intramolecular metal complexes ($M^{2+} = Cu^{2+}$, Co^{2+} and Ni^{2+}) and (b) chemical structure of peptoid oligomers **6P1**, **6P2**, **6P1Ac**, **6P2Ac**, **4P1**, **4P2**, **4P1Ac** and **4P2AC**.
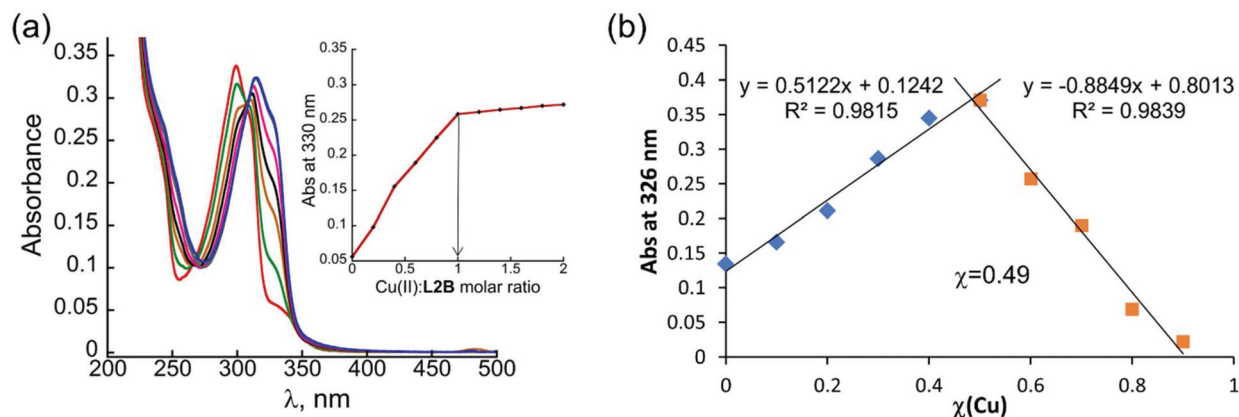

Fig. 2 (a) UV-Vis spectra and a metal-to-peptoid ratio plot for the titration of **L2B** with Cu^{2+} (17 μM) in acetonitrile. (b) Job-plot of **R-L2B** with Cu^{2+} measured in acetonitrile (33 μM total concentration).

chiometry ratios were 0.89 and 0.92 respectively. The formation of the intramolecular M(**peptoid**) complexes were verified in all cases by ESI-MS analysis (see ESI†).

Circular dichroism (CD) measurements revealed some changes in the region of 190–230 nm that corresponds to the secondary structure of the peptoid backbone, upon the formation of the complexes. PPI-type helical peptoids incorporating (S)-(−)-1-phenylethyl (Nspe) or (R)-(+)-1-phenylethyl (Nrpe) side-chains are typically characterized by double minima or double maxima, respectively, at about 200 and 220 nm. These bands are associated with the *trans* and *cis* amide bond conformations,[22] respectively, the later becoming the major conformation as the PPI-type peptoid helix is more stabilized in solution. The CD spectra of the metal-free peptoids **L2B** and **C3B** exhibit double minima near 200 and 220 nm, implying that they are folded into right-handed helices in solution, while **R-L2B** and **R-C3B** show double maxima near 200 and 220 nm, signifying that they are folded into left-handed helices in solution (Fig. 3). Upon addition of Cu^{2+}, Co^{2+} or Ni^{2+} to each peptoid, only minor differences in the intensity of the CD bands near 200 and 220 nm were observed (Fig. 3), suggesting that the overall conformational order of the peptoids is either slightly increased in the case of the linear peptoids or decreased in the case of the cyclic peptoids. These results are in agreement with our previously reported study in which Ru^{2+} was added to each of these four peptoids.[16] In contrast, metal binding to all three peptoids resulted in significant changes in the region between 280 to 360 nm. Bands in this region correspond to the π–π* transition of bipy, caused by the interaction between two bipy chromophores from the same backbone upon metal coordination. Specifically, addition of Cu^{2+}, Co^{2+} and Ni^{2+} to **L2B** resulted in a minimum CD signal at $\lambda_{max} =$ 332, 324 and 329 nm, respectively (Fig. 3a–c). The coordination of Cu^{2+}, Co^{2+} and Ni^{2+} by **C3B** also gave rise to new minimum

signals at $\lambda_{max} =$ 330, 322 and 328 nm, respectively, revealing the formation of chiral metal-bipy complexes (Fig. 3d–f). These signals reflect the induction of chirality from the peptoid scaffold to the metal center and indicate preferable stereochemistry of the Δ isomers over the Λ isomer,[23] as was observed in the case of the Ru^{2+} complex with **C3B**. In addition, the binding of Cu^{2+} and Ni^{2+} to **C3B** produced strong exciton couplet circular dichroism (ECCD) signals crossing $\varepsilon =$ 0 near 312 nm, demonstrating a high population of the isomers with Δ stereochemistry. The intensity of the exciton couplet signals from the Cu^{2+}, Co^{2+} and Ni^{2+} complexes with **C3B**, however, is higher than this of the analogue Ru^{2+} complex, especially in the case of Cu^{2+}, suggesting that there are some differences in the coordination geometry of the complexes.[2a] The CD spectra of the peptoids **R-L2B** and **R-C3B**, displayed the exact opposite spectra and cotton effect, following similar trends in all CD regions as the corresponding Nspe-based peptoids. Specifically, positive ECCD signals of the metal complexes, which represent a chiral induction to the metal center from the chiral peptoid scaffold, were observed. The complexes from the peptoid **R-C3B** correspond to the preferable Λ isomers (Fig. 3). These results demonstrate the transfer of chirality from a helical peptoid scaffold to embedded copper-, cobalt- and nickel-bipy complexes, which are at least 9 bonds away from a chiral center, and indicate that the stereochemistry of these metal complexes can be controlled by the chirality of the peptoid.

We next wished to explore whether the transfer of chirality from helical peptoids to metal centers is influenced by the type of incorporated side chains. To this aim, we first designed two hexamer peptoids **6P1** and **6P2**, analogues of **R-L2B** and **L2B**, bearing (R)-(−)-3,3-dimethyl-2-butylamine (Nr1tbe)[13] and (S)-(−)-1-(1-naphthyl)ethylamine (Ns1npe)[14] groups, respectively, instead of the Nspe groups (Fig. 1b). Previous studies
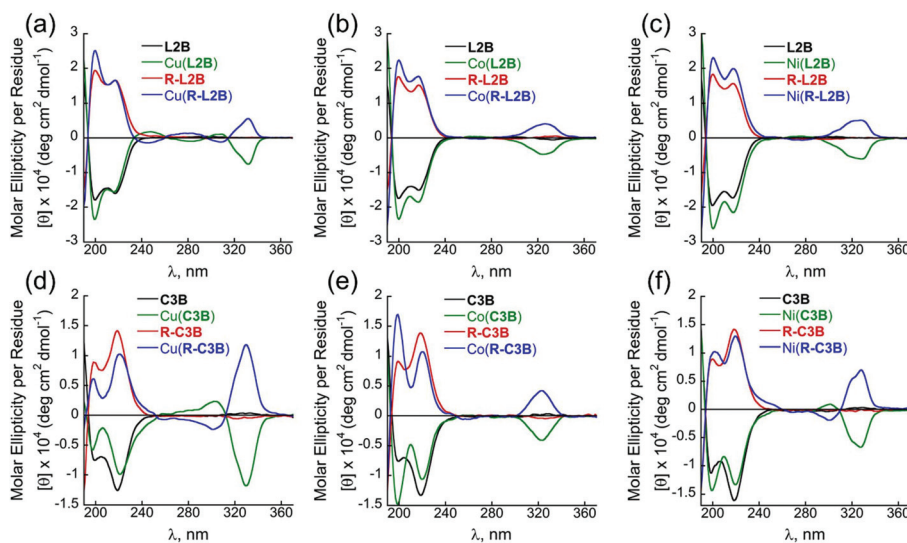

Fig. 3 CD spectra of the peptoid oligomers (a–c) **L2B**, **R-L2B**, (d–f) **C3B**, **R-C3B**, and their metal complexes measured at the concentration of 100 μM in acetonitrile.

demonstrated that both these side chains are excellent structure directing groups, for the construction of all-*cis* homo-oligomer PPI-type peptoids helices. Metal binding to helical peptoids containing these monomers, however, was not explored. The peptoids **6P1** and **6P2** were synthesized *via* the solid phase submonomer approach, cleaved and purified by HPLC (>95% purity) and their identity was confirmed by ESI-MS (see ESI†). The UV-Vis spectrum of **6P1** was similar to this of **L2B** and **R-L2B**, showing an absorbance band near $\lambda = 299$ nm. The UV-Vis spectrum of **6P2** revealed absorption bands at 272, 282 and 293 nm, which correspond to the superposition of absorptions of naphthyl and bipy moieties. Addition of metal ions to the free peptoid resulted in the disappearance of the bands corresponding to the bipy ligands and thus to a decrease in the intensity of the bands related to the naphthyl residues (Fig. S24–26†). UV-Vis titration experiments of **6P1** and **6P2** were conducted with Cu^{2+}, Co^{2+} and Ni^{2+} and suggested intramolecular binding with a ratio of 1 : 1 as obtained from the metal-to-peptoid ratio plots and from the Co(**6P1**) and Cu(**6P2**) Job plot experiments, which resulted in stoichiometry ratios of 0.89 and 0.92 respectively. The formation of 1 : 1 intramolecular M(**peptoid**) complexes were further confirmed by ESI-MS analyses of these metallopeptoids (see ESI†).

The CD spectrum of the free peptoid **6P1** exhibits a relatively weak signal with a minimum at 205 nm and maximum at 221 nm. This CD spectrum is a mirror image-like spectrum of a recently published helical *N*s1tbe-bearing homohexamer, exhibiting minimum near 225 nm and a maximum near 209 nm.[13] Upon addition of Cu^{2+} to the free peptoid **6P1**, the two CD bands diminished, suggesting that the helical structure is interrupted by the intramolecular coordination, probably due to the specific geometry the copper ion enforces on the overall peptoid structure (Fig. 4a).[19] Addition of Co^{2+}, however, resulted in a significant increase in the CD signal near 205 and 221 nm, demonstrating the stabilization of the helical structure upon metal binding (Fig. 4a).[18a] Similar effect was obtained by addition of Ni^{2+}, albeit with less intensity compare to Co^{2+}. Like in the case of the *N*rpe analogue peptoid **R-L2B**, the binding of Cu^{2+}, Co^{2+} and Ni^{2+} led to additional CD band centered at $\lambda_{max} = 332$, 325 and 330 nm, respectively, which reflect the transmission of the stereogenic

character of the peptoid scaffold to the metal center. The positive cotton effect in the far UV region indicated that **6P1** promotes a similar stereochemistry at the metal centers of the complexes it formed, as this of the metal complexes formed from **R-L2B**. Thus, the chirality of the side chains monomers, which directly dictates the handedness of the helicity, attributes to the chirality of the metal centers. CD spectra of the free peptoid **6P2** exhibits a strong CD signal with the minimum at 231 nm and maxima at 224 and 206 nm, corresponds to the pure PPI-like secondary structure.[14] Addition of the metal ions Cu^{2+}, Co^{2+} and Ni^{2+} to the free peptoid solution did not change significantly the CD spectra in the region of 190–240 nm, demonstrating that metal coordination has no effect on the conformational state of the peptoid oligomer (Fig. 4b). Similar to the *N*spe-based analogue peptoid **L2B**, Cu^{2+}, Co^{2+} and Ni^{2+} binding to **6P2** produced new CD bands with a negative cotton effect in the far UV region at $\lambda_{max} = 332$, 325 and 330 nm, respectively, which reflects the chiral induction from the peptoid to the embedded metal centers (Fig. 4b). Overall, these experiments reveal that the transfer of chirality from a helical peptoid to a metal center is not affected by the identity of the side chains.

It is known from previous studies that peptoids helicity is chain length dependent,[13,14,21] thus we wanted to further investigate whether the transfer of chiral information to the metal center can occur within peptoids short as tetramers, bearing only two chiral groups – the minimum requires to keep the two bipy ligands in the *i* and *i* + 3 positions. To this aim, we modified **6P1** and **6P2** by synthesizing their tetramer analogues **4P1** and **4P2** (Fig. 1b). UV-Vis titration of these tetramers with Cu^{2+}, Co^{2+} and Ni^{2+} suggested intramolecular binding with a ratio of 1 : 1 as obtained from the metal-to-peptoid ratio plots and from the Job plots of Co(**4P1**) and Ni(**4P2**), which resulted in stoichiometry ratios of 0.79 and 1.01 respectively. The formation of intramolecular complexes was further confirmed by ESI-MS analysis (see ESI†). Although the CD spectra of **4P1** in the region between 190–240 nm was similar to the CD spectra of **6P1** in the same region, the two bands at 205 and 221 nm, characteristic of the helical structure of **4P1**, diminished upon addition of all three metal ions (Fig. S40†), suggesting that the conformational order is reduced by metal coordination. In contrast, addition of all three metal ions to **4P2**, which its CD spectra in the region between 190–240 nm was similar to the CD spectra of **6P2** in the same region, resulted in a significant increase in the CD signal near 231 nm, and the band near 224 nm disappeared (Fig. S41†). These observations suggest that metal coordination to **4P2** enhances its conformational order and assists in stabilizing its helical structure.

Interestingly, the CD spectra of these two peptoids and their complexes with the metal ions Cu^{2+}, Co^{2+} and Ni^{2+} did not produce CD signals in the region related to the π–π* transition of the bipy ligand, demonstrating that the metal complexes formed are not chiral, namely there is no chiral induction from the peptoid to the metal centers (Fig. S40 and 41†). One reason for this lack of chiral induction could be simply a
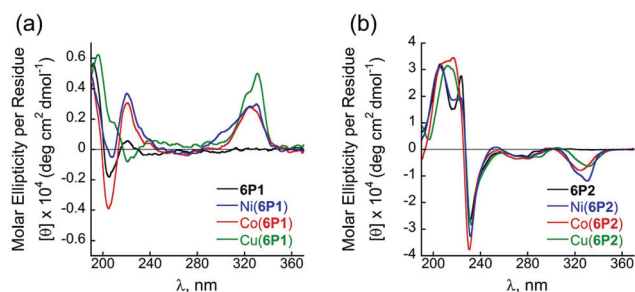

Fig. 4 CD spectra of the peptoid oligomers (a) **6P1** and (b) **6P2** and their metal complexes measured at the concentration of 100 μM in acetonitrile.

consequence of these peptoids bearing only two chiral groups. Another possible reason might be the different binding modes of the tetramers compare to the hexamers due to the different locations of one bipy ligand – either near the terminal secondary amine (tetramers) or far from it (hexamers). It is known that N–H groups can participate in the binding of metal ions. Thus, if the N–H group of **4P1** is involved in metal binding because it is located near the metal center, but is not involved in metal binding within **6P1** because it is too far from the metal center, then the two complexes will have different coordination geometries, resulting an achiral complex in the case of **4P1** and a chiral one in the case **6P1**. In order to evaluate whether the terminal N–H group is involved in the binding, we recorded the FTIR spectra of the peptoids **4P1** and **6P1** and of their Cu^{2+} complexes. The resulted spectrum of **4P1** shows a band near 3370 cm^{-1}, corresponding to the N–H stretching. This band, however, is not present in the FTIR spectrum of Cu(**4P1**) complex (Fig. S44†), supporting the assumption that the intramolecular metal coordination involves the N-terminus amine. In contrast, the FTIR spectra of **6P1** and Cu(**6P1**) exhibit bands near 3380 and 3322 cm^{-1}, respectively (Fig. S45†), indicating that the terminal N–H group is not involved in the metal binding.

To support this further and to explore the possibility of recovering the chiral induction, we decided to acetylate the N-terminus amine in peptoids **4P1** and **4P2** and generate their corresponding acetylated prototypes peptoids **4P1Ac** and **4P2Ac** (Fig. 1b). By this we thought to eliminate the formation of the undesired coordination geometry that leads to achiral complexes. The peptoids **4P1Ac** and **4P2Ac** were synthesized on solid support, cleaved from resin, purified by HPLC (>95% purity) and their identity was confirmed by ESI-MS analysis. Their CD spectra before and after Cu^{2+} addition were recorded and compared with their non-acetylated prototypes. The CD spectrum of the free **4P1Ac** exhibits a weak signal with maxima at 195 and 220 nm and minimum at 206 nm. Upon addition of metal ions, additional CD bands at the region that corresponds to the bipy ligand transitions appeared, indicating chiral induction to the metal center. The metallopeptoid complexes Co(**4P1Ac**) and Ni(**4P1Ac**) display similar CD bands as

the complexes of **6P1**, with a positive cotton effect, centered at λ_{max} = 323 and 309 nm, respectively (Fig. 5a). Surprisingly, upon addition of Cu^{2+} to the free peptoid **4P1Ac** a strong CD band at λ_{max} = 330 nm appeared, with a negative cotton effect rather than the expected positive band. This band is twice more intense than the corresponding CD band of Cu(**6P1**) complex with the opposite CD sign, demonstrating that different chirality of the complex was obtained. This result indicates that the acetylation of the N-terminus influenced dramatically the geometry of the Cu^{2+} complex, resulting in the opposite chirality. In addition, coordination of Cu^{2+} and Co^{2+} to **4P1Ac** resulted in a dramatic increase of the CD intensity in the region between 190–240 nm, suggesting a significant stabilization of the helical structure by metal coordination.

Free peptoid **4P2Ac** displays CD signals with maxima at λ_{max} = 207 and 226 nm and minima at λ_{max} = 220 and 234 nm. The CD bands in this region almost did not change upon addition of Cu^{2+} but the intensity increased significantly after binding of Co^{2+} and Ni^{2+} (Fig. 5b), suggesting conformational stabilization of the peptoid scaffold *via* metal coordination. In addition to that, metal binding by **4P2Ac** resulted in CD bands in the region of 280–360 nm with a similar shape and position but slightly higher intensity as the hexamer peptoid **6P2**, demonstrating the chiral induction from the peptoid to each metal center. These results indicate that the acetylation of the N-terminus have a dramatic influence on the binding mode of **4P1** and **4P2**. These outcomes support the assumption that the terminal N–H has a contribution to the metal coordination of the peptoids **4P1** and **4P2**, resulting in the loss of chirality of the metal centers.

Following these observations, we decided to explore how N-terminus acetylation affects the chiral induction ability of the peptoid hexamers **6P1** and **6P2** on the different metal centers. To this aim, we synthesized on solid support the corresponding acetylated **6P1Ac** and **6P2Ac** peptoids *via* the submonomer approach, and they as well were cleaved from the resin, purified by HPLC (>95% purity) and their masses were confirmed by MS analysis. The CD spectra of **6P2Ac** and its metal complexes are very similar to these of the non-acetylated analogue **6P2**, demonstrating that the acetylation of the
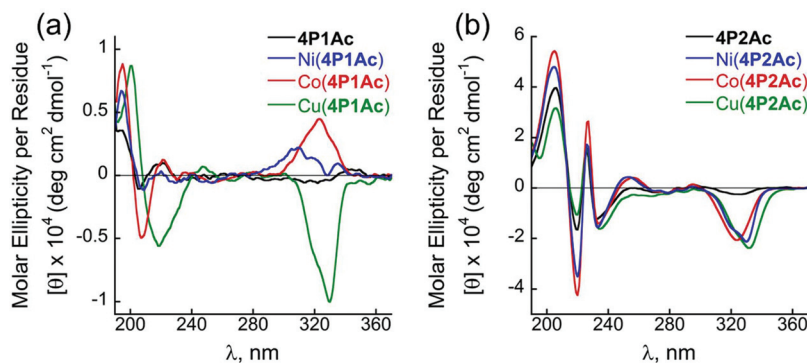

Fig. 5 CD spectra of the peptoid oligomers (a) **4P1Ac** and (b) **4P2Ac** and their metal complexes measured at the concentration of 100 μM in acetonitrile.

N-terminus has little or no effect on the chiral induction process in this peptoid (Fig. S43†). The CD spectra of **6P1Ac** and its Cu^{2+} complex are also very similar to these of **6P2** (Fig. S42†). Surprisingly, the complexes Co(**6P1Ac**) and Ni (**6P1Ac**) seem different from the corresponding complexes of **6P1**, as no chiral induction was observed in their CD spectra (Fig. S42†). Within the peptoid hexamers, the secondary amine at the termini is located relatively far from the metal center; thus, metal coordination by the N–H group in these peptoids is less possible, as was also implied by the FTIR analysis. Therefore, the loss of chirality at the metal center could be a consequence of steric and/or electronic effects attributed to the acetylation, which might induce changes on the coordination geometry of the metal center, resulting in the loss of chirality.

Conclusions

To sum up, this work describes the intramolecular binding of Cu^{2+}, Co^{2+} and Ni^{2+} within previously designed as well as new bipy modified helical peptoids. Eight hexamers and four tetramers, each from a different type of structure directing element, namely, *N*spe, *N*rpe, *N*s1npe or *N*r1tbe, with distinct stereogenic centers, were examined for their ability to transfer their chirality to embedded achiral metal centers. We found that in most cases there is chiral induction from the peptoid backbone to each metal center. We first show that by changing the chirality of the side groups (*S* or *R*) we can control the chirality of the formed metal centers. By reducing the length of the peptoid sequence to only four monomers, we could obtain chiral metal complexes after acetylation of the N-terminus amine. These results demonstrate that even in a very short peptoid length, a chiral induction from the peptoid scaffold and control over the stereochemistry of metal centers can be achieved. Finally, we advocate that the coordination environment about the metal center, which is controlled by the identity of the N-terminus, has a significant effect on the ability of the peptoids to transfer their chirality to the metal centers. We believe that this work opens up wide prospects for the design of chiral metallopeptides towards biomimetic and chemical applications. Our current efforts target long distance transfer of chirality (remote chiral induction) as well as enantioselective catalysis.

Experimental section

Materials

Rink amide resin was purchased from Novabiochem; trifluoroacetic acid (TFA) and nickel acetate tetrahydrate were purchased from Alfa Aesar; (*S*)-(−)-1-phenylethylamine, (*R*)-(+)-1-phenylethylamine and (*S*)-(−)-1-(1-naphthyl)ethylamine were purchased from Acros; bromoacetic acid, cobalt acetate tetrahydrate and copper acetate monohydrate were purchased from MERCK; *N*,*N*′-diisopropylcarbodiimide (DIC), piper-

idine, 6-bromo-2,2′-bipyridine, (*R*)-(−)-3,3-dimethyl-2-butylamine, acetonitrile (ACN) and water HPLC grade solvents were purchased from Sigma-Aldrich; dimethylforamide (DMF) and dichloromethane (DCM) solvents were purchased from Bio-Lab Ltd. 2-(2,2′-Bipyridine-6-yloxy) ethylamine (*N*bp) was synthesized according to previously published procedure.[16]

Instrumentation

Peptoid oligomers were analyzed by reversed-phase High-performance liquid chromatography (HPLC) using analytical C18(2) column, Phenomenex, Luna 5 μm, 100 Å, 2.0 × 50 mm, on a Jasco UV-2075 PLUS detector. Purification of peptoid oligomers was performed by preparative HPLC using AXIA Packed C18(2) column, Phenomenex, Luna 15μm, 100 Å, 21.20 × 100 mm. Mass spectrometry of peptoid oligomers was performed on Advion expression CMS mass spectrometer under electrospray ionization (ESI), direct probe with ACN, flow rate 0.2 ml min⁻¹. Analysis of metal complexes was performed on Waters Acquity and on Waters LCT Premier mass spectrometers under electrospray ionization (ESI), direct probe ACN : H_2O (70 : 30), flow rate 0.3 ml min⁻¹. UV measurements were carried out using an Agilent Cary 60 UV-Vis spectrophotometer. FTIR measurements were recorded on Agilent Cary 630 FTIR spectrometer equipped with a diamond attenuated total reflection (ATR). CD measurements were performed using a circular dichroism spectrometer Applied Photophysics Chirascan. Data processing was done with the softwares Excel and KaleidaGraph.

Synthesis and purification of the peptoid oligomers

Solid-phase synthesis of peptoid oligomers was carried out manually in fritted syringes on Rink amide resin at room temperature using the previously reported peptoid submonomer protocol.[24] Peptoid synthesis was performed with alternating bromoacylation and amine displacement steps until peptoid oligomers of desired sequence were obtained. Acetylation of the peptoids performed by mixing DIC (2 ml for g⁻¹ resin) with Acetic acid (8.5 ml 1.2 M for g⁻¹ resin) for 1 h. After the peptoid synthesis, the products were cleaved from the resin by treatment with 95% trifluoroacetic acid (TFA) in water (50 mL g⁻¹ resin) for 30 minutes. The cleavage mixture was concentrated in vacuum and cleaved samples were then re-suspended in 50% acetonitrile in water and lyophilized to powders. Afterwards, crude peptoids were dissolved in 50% acetonitrile in water and purified by preparative HPLC (C18 column). Products were detected by UV absorbance at 230 nm during a linear gradient conducted from 5% to 95% solvent B (0.1% TFA in HPLC grade acetonitrile) over solvent A (0.1% TFA in HPLC grade water) in 50 minutes with a flow rate of 5 mL min⁻¹. Purified products were analyzed by reversed-phase HPLC (C18 column) with a linear gradient of 5–95% ACN in water (0.1% TFA) over 10 min at a flow rate of 0.7 mL min⁻¹ and 214 nm UV absorbance.

Circular dichroism

CD measurements were performed at room temperature at concentration of 100 μM in solution of ACN. The spectra were obtained by averaging 4 scans per sample in a fused quartz cell (path length = 0.1 cm), over the 370 to 190 nm region at a step of 1 nm (scan rate = 1 s per step). In a typical experiment the CD of free peptoid was first measured followed by addition of 1.2 equiv. of metal ion solution and the sample was measured again.

UV-VIS spectroscopy

Titration experiments of the peptoid oligomers with the metal ions (Co^{2+}, Cu^{2+} and Ni^{2+}) were followed by UV-Vis analysis in ACN solution using 17 μM concentration. In a typical experiment, 10 μL of a peptoid solution (5 mM in ACN) were diluted in 3 ml ACN solution and then titrated in multiple steps with 2 μL aliquots of a metal ion (5 mM in H_2O) until the binding was completed. Job plot experiments were determined using UV-Vis spectrometry by varying mole fraction of metal ions and peptoid oligomers using 26–66 μM total molar concentration in ACN solution.

Synthesis of metal complexes for MS analysis

A solution of peptoid oligomers (100–200 μL 0.5 mM) in ACN was treated with metal solution (5 mM in H_2O) and the mixture was stirred for 30 minutes prior to MS analysis.

Conflicts of interest

There are no conflicts to declare.

Acknowledgements

Notes and references

1 L. Byrne, J. Sol, T. Boddaert, T. Marcelli, R. W. Adams, G. A. Morris and J. Clayden, *Angew. Chem., Int. Ed.*, 2014, **126**, 155–159.

2 (*a*) G. Pescitelli, L. Di Bari and N. Berova, *Chem. Soc. Rev.*, 2014, **43**, 5211–5233; (*b*) N. Ouaka, Y. Takeyama, H. Lida and E. Yashima, *Nat. Chem.*, 2011, **3**, 856–861.

3 (*a*) D. J. Hill, M. J. Mio, R. B. Prince, T. S. Hughes and J. S. Moore, *Chem. Rev.*, 2001, **101**, 3893–4011.

4 G. Guichard and I. Huc, *Chem. Commun.*, 2011, **47**, 5933–5941.

5 (*a*) S. H. Gellman, *Acc. Chem. Res.*, 1998, **31**, 173–180; (*b*) D. Seebach and J. Cardiner, *Acc. Chem. Res.*, 2008, **41**, 1366–1375.

6 J. Crassous, *Chem. Commun.*, 2012, **48**, 9684–9692.

7 M. Baskin and G. Maayan, *Chem. Sci.*, 2016, **7**, 2809–2820.

8 (*a*) O. Gidron, M. O. Ebert, N. Trapp and F. Diederich, *Angew. Chem., Int. Ed.*, 2014, **53**, 13614–13618; (*b*) A. G. Petrovic, G. Vantomme, Y. L. Negrón-Abril, E. Lubian, G. Saielli, I. Menegazzo, R. Cordero, G. Proni, K. Nakanishi, T. Carofiglio and N. Berova, *Chirality*, 2011, **23**, 808–819.

9 (*a*) G. Maayan, M. D. Ward and K. Kirshenbaum, *Proc. Natl. Acad. Sci. U. S. A.*, 2009, **106**, 13679–13684; (*b*) R. Schettini, F. De Riccardis, G. Della Sala and I. Izzo, *J. Org. Chem.*, 2016, **81**, 2494–2505.

10 A. S. Knight, E. Y. Zhou, M. B. Francis and R. N. Zuckermann, *Adv. Mater.*, 2015, **27**, 5665–5691.

11 P. J. Kaniraj and G. Maayan, *Org. Lett.*, 2015, **17**, 2110–2113.

12 (*a*) K. Kirshenbaum, A. E. Barron, R. A. Goldsmith, P. Armand, E. Bradley, K. T. V. Truong, K. A. Dill, F. E. Cohen and R. N. Zuckermann, *Proc. Natl. Acad. Sci. U. S. A.*, 1998, **95**, 4303–4308; (*b*) C. W. Wu, T. J. Sanborn, K. Huang, R. N. Zuckermann and A. E. Barron, *J. Am. Chem. Soc.*, 2001, **123**, 6778–6784; (*c*) C. W. Wu, K. Kirshenbaum, T. J. Sanborn, J. A. Patch, K. Huang, K. A. Dill, R. N. Zuckermann and A. E. Barron, *J. Am. Chem. Soc.*, 2003, **125**, 13525–13530; (*d*) B. C. Gorske, B. L. Bastian, G. D. Geske and H. E. Blackwell, *J. Am. Chem. Soc.*, 2007, **129**, 8928–8929; (*e*) N. H. Shah, G. L. Butterfoss, K. Nguyen, B. Yoo, R. Bonneau, D. L. Rabenstein and K. Kirshenbaum, *J. Am. Chem. Soc.*, 2008, **130**, 16622–16632; (*f*) B. C. Gorske, J. R. Stringer, B. L. Bastian, S. A. Fowler and H. E. Blackwell, *J. Am. Chem. Soc.*, 2009, **131**, 16555–16567; (*g*) O. Roy, C. Caumes, Y. Esvan, C. Didierjean, S. Faure and C. Taillefumier, *Org. Lett.*, 2013, **15**, 2246–2249; (*h*) C. Caumes, O. Roy, S. Faure and C. Taillefumier, *J. Am. Chem. Soc.*, 2012, **134**, 9553–9556; (*i*) B. C. Gorske, E. M. Mumford, C. G. Gerrity and I. Ko, *J. Am. Chem. Soc.*, 2017, **139**, 8070–8073.

13 O. Roy, G. Dumonteil, S. Faure, L. Jouffret, A. Kriznik and C. Taillefumier, *J. Am. Chem. Soc.*, 2017, **139**, 13533–13540.

14 (*a*) J. R. Stringer, J. A. Crapster, I. A. Guzei and H. E. Blackwell, *J. Am. Chem. Soc.*, 2011, **133**, 15559–15567; (*b*) J. A. Crapster, I. A. Guzei and H. E. Blackwell, *Angew. Chem., Int. Ed.*, 2013, **52**, 5079–5084.

15 (*a*) B. C. Lee, T. K. Chu, K. A. Dill and R. N. Zuckermann, *J. Am. Chem. Soc.*, 2008, **130**, 8847–8855; (*b*) N. Maulucci, I. Izzo, G. Bifulco, A. Aliberti, C. De Cola, D. Comegna, C. Gaeta, A. Napolitano, C. Pizza, C. Tedesco, D. Flot and F. De Riccardis, *Chem. Commun.*, 2008, 3927–3929; (*c*) C. De Cola, S. Licen, D. Comegna, E. Cafaro, G. Bifulco, I. Izzo, P. Tecilla and F. De Riccardis, *Org. Biomol. Chem.*, 2009, **7**, 2851–2854; (*d*) G. Della Sala, B. Nardone, F. De Riccardis and I. Izzo, *Org. Biomol. Chem.*, 2013, **11**, 726–731; (*e*) I. Izzo, G. Ianniello, C. De Cola, B. Nardone, L. Erra, G. Vaughan, C. Tedesco and F. De Riccardis, *Org. Lett.*,

2013, **15**, 598–601; (*f*) C. De Cola, G. Fiorillo, A. Meli, S. Aime, E. Gianolio, I. Izzo and F. De Riccardis, *Org. Biomol. Chem.*, 2014, **12**, 424–431; (*g*) C. Tedesco, L. Erra, I. Izzo and F. De Riccardis, *CrystEngComm*, 2014, **16**, 3667–3687; (*h*) T. Zabrodski, M. Baskin, J. K. Prathap and G. Maayan, *Synlett*, 2014, A–F; (*i*) A. S. Knight, E. Y. Zhou, J. G. Pelton and M. B. Francis, *J. Am. Chem. Soc.*, 2013, **135**, 17488–17493; (*j*) A. S. Knight, E. Y. Zhou and M. B. Francis, *Chem. Sci.*, 2015, **6**, 4042–4048; (*k*) K. J. Prathap and G. Maayan, *Chem. Commun.*, 2015, **51**, 11096–11099; (*l*) E. De Santis, A. A. Edwards, B. D. Alexander, S. J. Holder, A.-S. Biesse-Martin, B. V. Nielsen, D. Mistry, L. Waters, G. Siligardi, R. Hussain, S. Faurede and C. Taillefumier, *Org. Biomol. Chem.*, 2016, **14**, 11371–11380.

16 M. Baskin, L. Panz and G. Maayan, *Chem. Commun.*, 2016, **52**, 10350–10353.

17 (*a*) G. Maayan, *Eur. J. Org. Chem.*, 2009, 5699–5710; (*b*) E. G. Maayan and M. Albrecht, in *Metallofoldamers. Supramolecular Architectures from Helicates to biomimetics*, John Wiley& Sons, Ltd, 2013; (*c*) F. Zhang, S. Bai, G. P. A. Yap, V. Tarwade and J. M. Fox, *J. Am. Chem. Soc.*, 2005, **127**, 10590–10599; (*d*) Z. Dong Jr., R. J. Karpowicz, S. Bai, G. P. A. Yap and J. M. Fox, *J. Am. Chem. Soc.*, 2006, **128**, 14242–14243; (*e*) Y. Zhao and Z. Zhong, *J. Am. Chem. Soc.*, 2006, **128**, 9988–9989; (*f*) R. Métivier, I. Leray and B. Valeur, *Chem. – Eur. J.*, 2004, **10**, 4480–4490; (*g*) Y. Zhao and Z. Zhong, *Org. Lett.*, 2006, **8**, 4715–4717; (*h*) G. Lelais, D. Seebach, B. Jaun, I. Raveendra, R. I. Mathad, O. Flögel, F. Rossi, M. Campo and A. Wortmann, *Helv. Chem. Acta*,

2006, **89**, 361–403; (*i*) C. E. Schafmeister, L. G. Belasco and P. H. Brown, *Chem. – Eur. J.*, 2008, **14**, 6406–6412; (*j*) Z. Ma, Y. A. Skorik and C. Achim, *Inorg. Chem.*, 2011, **50**, 6083–6092; (*k*) S. Tashiro, K. Matsuoka, A. Minoda and M. Shionoya, *Angew. Chem., Int. Ed.*, 2012, **51**, 13123–13127; (*l*) J. P. Miller, M. S. Melicher and A. Schepartz, *J. Am. Chem. Soc.*, 2014, **136**, 14726–14729.

18 (*a*) G. Maayan, M. D. Ward and K. Kirshenbaum, *Chem. Commun.*, 2009, 56–58; (*b*) M. Baskin and G. Maayan, *Biopolymers*, 2015, **104**, 577–584.

19 L. Zborovsky, A. Smolyakova, M. Baskin and G. Maayan, *Chem. – Eur. J.*, 2018, **24**, 1159–1167.

20 Stoichiometry ratio (*a*) was determined by calculation the intersection point from the two equations:
$$a = \frac{\chi_M}{1 - \chi_M} = \frac{0.49}{0.51} \cong 1.$$

21 J. S. Renny, L. L. Tomasevich, E. H. Tallmadge and D. B. Collum, *Angew. Chem., Int. Ed.*, 2013, **52**, 11998–12013.

22 C. W. Wu, T. J. Sanborn, R. N. Zuckermann and A. E. Barron, *J. Am. Chem. Soc.*, 2001, **123**, 2958–2963.

23 (*a*) M. H. Filby, J. Muldoon, S. Dabb, N. C. Fletcher, A. E. Ashcroft and A. J. Wilson, *Chem. Commun.*, 2011, **47**, 559–561; (*b*) I. Gamba, G. Rama, E. Ortega-Carrasco, R. Berardozzi, V. M. Sánchez-Pedregal, L. Di Bari, J.-D. Maréchal, M. E. Vázquez and M. V. López, *Dalton Trans.*, 2016, **45**, 881–885.

24 R. N. Zuckermann, J. M. Kerr, S. B. W. Kent and W. H. Moosm, *J. Am. Chem. Soc.*, 1992, **114**, 10646–10647.